



Original Article

Synergistic Adhesiveness of Fibronectin with PHSRN Peptide in Gelatin Mixture Promotes the Therapeutic Potential of Human ES-Derived MSCs

HYE-SEON KIM,¹ SUNG HYUN CHOI,² MI-LAN KANG,¹ KI-WON LEE,¹ KI NAM KIM,²
and HAK-JOON SUNG ¹

¹Department of Medical Engineering, Yonsei University College of Medicine, Seoul 03722, Republic of Korea; and ²Cellular Therapeutics Team, Daewoong Pharmaceutical, Yongin 17028, Gyeonggi-do, Republic of Korea

(Received 10 August 2019; accepted 13 November 2019; published online 2 December 2019)

Associate Editor Michael R. King oversaw the review of this article.

Abstract

Introduction—Mesenchymal stem cells (MSCs) are promising candidates for cell therapy owing to their therapeutic effect in various diseases. In general, MSCs grow efficiently in serum-containing culture media, indicating an essential role of adhesion in their mesenchymal lineage-specific propagation. Nevertheless, the use of non-human supplements in culture (xeno-free issue) in addition to the lack of control over unknown factors in the serum hampers the clinical transition of MSCs.

Methods—In this study, embryonic stem cell derived mesenchymal stem cells (ES-MSCs) were used owing to their scalable production, and they expressed a series of MSC markers same as adipose-derived MSCs. The affinity of the culture matrix was increased by combining fibronectin coating with its adjuvant peptide, gelatin, or both (FNGP) on tissue culture polystyrene to compare the regenerative, therapeutic activities of ES-MSCs with a cell binding plate as a commercial control.

Results—The FNGP culture plate promoted pivotal therapeutic functions of ES-MSCs as evidenced by their increased stemness as well as anti-inflammatory and proangiogenic effects *in vitro*. Indeed, after culturing on the FNGP plates, ES-MSCs efficiently rescued the necrotic damages in mouse ischemic hindlimb model.

Conclusions—This study suggests a potential solution by promoting the surface affinity of culture plates using a mixture of human fibronectin and its adjuvant PHSRN peptide in gelatin. The FNGP plate is expected to serve as an

effective alternative for serum-free MSC expansion for bench to clinical transition.

Keywords—ES-MSC, Serum-free expansion, PHSRN, Fibronectin, Gelatin.

ABBREVIATIONS

MSC	Mesenchymal stem cells
ES	Embryonic stem cell
ES-MSCs	Embryonic stem cell-derived mesenchymal stem cells
FN	Fibronectin
FNG	Fibronectin coating with gelatin
FNP	Fibronectin coating with adjuvant peptide PHSRN
FNGP	Fibronectin coating with gelatin and adjuvant peptide PHSRN
TCP	Tissue culture plate
TCPS	Tissue culture plate polystyrene
CB	CellBind®
PHSRN	Pro-His-Ser-Arg-Asn
ADSC	Adipose derived mesenchymal stem cell
ROS	Residual reactive oxygen species
KLF4	Kruppel-like factor 4
NANOG	Homeobox protein nanog
SOX2	Sex determining region Y-box 2
APEX1	Apurinic/apyrimidinic endonuclease 1
SENS1	Scalp-ear-nipple syndrome
SOD2	Superoxide dismutase 2
TXN	Thioredoxin
HUVEC	Human umbilical vein endothelial cells
IL-10	Interleukin 10
IL-6	Interleukin 6

Address correspondence to Hak-Joon Sung, Department of Medical Engineering, Yonsei University College of Medicine, Seoul 03722, Republic of Korea; Ki Nam Kim, Cellular Therapeutics Team, Daewoong Pharmaceutical, Yongin 17028, Gyeonggi-do, Republic of Korea. Electronic mails: 7107140@daewoong.co.kr and HJ72SUNG@yuhs.ac

Hye-Seon Kim, Sung Hyun Choi and Ki Nam Kim have contributed equally to this work.

ELISA	Enzyme-linked immunosorbent assay
DMEM	Dulbecco's modified Eagle's medium
FBS	Fetal bovine serum
PS	Penicillin streptomycin
CCK-8	Cell counting kit-8
qPCR	Real time quantitative PCR
GAPDH	Glyceraldehyde 3-phosphate dehydrogenase
RGD	Arg-Gly-Asp
RFP	Red fluorescent protein
EB	Embryonic body

INTRODUCTION

The growth and differentiation of mesenchymal stem cells (MSCs) are regulated by surface adhesiveness of the culture plates. Emerging evidence suggests that this structure–function relationship is governed by several crucial factors such as fibronectin concentration, integrin type and spacing, and cytoskeleton behavior.⁶ The spreading of adhesive MSCs to a large area triggers osteogenic differentiation of MSCs, whereas non-spreading, less adhesive morphologies are dominant during their adipogenic differentiation. Although there has been continuous progress in the research regarding this field, MSC type-specific information has not yet been fully elucidated. Moreover, MSCs spontaneously differentiate to unexpected lineages,³³ and maintaining the native phenotype of MSCs *via* cell–material interaction has been relatively underexplored compared to their directed differentiation. Collectively, MSC type-specific study on the adhesiveness in culture is required to preserve their *in vivo* characteristics, and thus the development of culture substrates that maintain stemness (i.e., the ability of a stem cell to both self-renew and differentiate) is crucial for the successful clinical applications of MSCs. Nevertheless, few recent studies have investigated the changes in human MSC (hMSC) stemness in response to material and biochemical cues and have suggested substrates that can maintain an undifferentiated state of hMSCs with high therapeutic potential.^{10,24}

hMSCs were subjected to several clinical trials to evaluate their therapeutic efficacy for various applications.²² However, their clinical potential has been limited, in part, because exhaustive *in vitro* expansion of hMSCs to achieve transplantable numbers causes cell senescence-associated abnormalities. Recent studies suggest embryonic stem cell (ES) as a potential cell source to provide infinite MSCs because ES-derived MSCs (ES-MSCs) possess similar characteristics to

bone marrow-derived MSCs with respect to differentiation potential, immunomodulatory function, and proangiogenic activity.^{8,9} Three of the most popular methods⁹ to derive MSCs from ES are (i) the use of embryonic body (EB) in a form of cell aggregate with addition of special culture medium and growth factors; (ii) the use of feeder cell layer; and (iii) the use of adhesive ECM components. Among others, this study focused on the third method owing to the commercial availability of cell binding plates, lower production of heterogeneous cell populations than those produced using EB, and the reduced labor and easier processes during production compared to the feeder cell method. Considering the use of cell aggregates in a hanging-drop status for ES culture, the use of adhesive culture plates for MSC culture indicates a key role of matrix affinity in maintaining the MSC characteristics.

For clinical trials in early 2000s, the use of fetal calf serum for hMSC culture was approved by FDA.^{19,31} However, xeno-source serum caused mycoplasma infection. Microbial infection and immune rejection when hMSCs were transplanted. The use of non-human supplements in culture in addition to the lack of control over unknown factors in the serum hampers the clinical transition of MSCs.^{21,26,32} Hence, xeno-free culture of hMSCs in GMP facilities has been tried due to the reduced complication rate. In this study, as cell adhesion plays an essential role in mesenchymal lineage-specific propagation of ESCs, the affinity of the culture matrix was increased by combining fibronectin (FN) coating with its adjuvant peptide (FNP), gelatin (FNG), or both (FNGP) on tissue culture polystyrene (TCP) to compare the MSC-EC behavior with a cell binding plate (CB) as a commercial control. CB plate (Corning CellBind® surface product, Corning Co., Ltd) is produced by treating atmospheric/vacuum plasma to the surface of tissue culture vessel. As a result, the amount of aromatic group decreases whereas the number of reactive groups (C–O–C, C=O, COOH/R) increases in the polystyrene backbone. The functional groups increased wettability and hydrophilicity, thereby promoting protein adsorption and cell attachment.¹ These test groups were selected because RGD(Arg-Gly-Asp) played a pivotal role in FN affinity, and the copresence of RGD and PHSRN (Pro-His-Ser-Arg-Asn) adjuvant peptides increased the ECM affinity compared to RGD alone.³ In addition, gelatin served as a coating mixture bed for the affinity components. ES-MSCs were cultured post-deposition of human FN and/or human sequence PHSRN in gelatin without using any animal serum.

After culturing on the test culture plates, the adhesion/growth, stemness, and proangiogenic/anti-inflammatory activities of ES-MSCs were determined. The results suggest FNGP as a promising candidate to

improve their therapeutic potential. Importantly, when these groups were implanted into the damage sites in mouse ischemic hindlimbs, the FNGP group promoted blood perfusion, thereby regenerating the necrotic tissues.

MATERIALS AND METHODS

Culture of ADSC and ES-MSC

ADSCs (5×10^5 cells/mL) were purchased from PromoCell (Heidelberg, Germany) and propagated on 150 π tissue culture plate polystyrene (TCPS) in low-glucose Dulbecco's modified Eagle's medium (DMEM, Gibco, USA) supplemented with 10% fetal bovine serum (FBS, Gibco, USA) and 1% penicillin-streptomycin (PS, Gibco, USA). Human embryonic stem cell-derived mesenchymal stem cells (ES-MSCs, 5×10^5 cells/mL) were provided by Daewoong Pharmaceutical Co., Ltd. (Republic of Korea). The transition for ES to MSC was confirmed, and ES-MSCs were used by propagating serially until passage 8 on 175T CellBind® (CB) plate in a StemPro® MSC SFM XenoFree (Gibco, USA) supplemented with 1% L-glutamine (Gibco, USA). All cell cultures were incubated with 7.5% CO₂ at 37 °C.

Flow Cytometry

ADSC (passage 2) and ES-MSC (passage 10 and 11) were detached and washed with PBS (Phosphate-Buffered Saline, Welgene, Republic of Korea) thrice, followed by Flow cytometry analysis using human MSC analysis kit (BD Bioscience, USA), according to the manufacturer's instruction. Cells were reacted with antibodies of CD73^{APC}, CD44^{PE}, or negative cocktail^{PE} (mixture of CD34, CD11b, CD19, CD45, and HLA-DR) for 1 h at room temperature (RT) using a 360° reverse rotator and were then centrifuged for 3 min at 1300 rpm. The pellets were suspended in 1 mL PBS and then run into Flow Cytometer (BD FACSTM, BD Bioscience) *via* data analysis using CellQuest-Pro (BD Bioscience).

Test Culture Plates

Porcine skin derived gelatin powder (Sigma-Aldrich, USA) was dissolved in sterile PBS (1% w/v) and filtered using a tube top vacuum filter (0.22 μ m pore size, Corning, USA).²³ Human fibronectin (Gibco, USA) and PHSRN (Lugen Sci Co., Ltd., Republic of Korea) were diluted in sterile PBS to 5 μ g/mL and 100 μ M,¹⁷ respectively. Either mixture solution of gelatin and fibronectin (1:1) or fibronectin only was coated into

TCPS by incubating for 2 h at 37 °C, followed by PBS washing and further coating with PHSRN solution for 2 h at 37 °C. The test culture plates include fibronectin only (FN), fibronectin with gelatin (FNG), fibronectin with PHSRN (FNP), FNG with PHSRN (FNGP), and cell bind (CB) plate (a commercial control).

Cell Morphology and Proliferation

ES-MSC (5×10^3 cells/mL) were propagated on CellBind® 24 well clear multiple plate and FNGP coated 24 well culture plate. Attached cell morphologies were visualized by actin staining. Cells were fixed in a 4% paraformaldehyde solution and were permeabilized with 0.3% triton X-100 (Sigma-Aldrich) for 10 min. Cells were then washed with PBS and treated with Phalloidin 594 (1:1000, Abcam, UK) for 1 h at RT with nucleus counterstaining in NucBlue Fixed Cell ReadyProbes Reagent (Thermo Fisher Scientific, USA). Samples were subjected to fluorescence imaging (Leica, Germany). Cell proliferation was determined on Days 1, 4, and 7 post-seeding by incubating ES-MSC (5×10^3 cell/well in a 24-well plate) with cell counting kit-8 solution (CCK-8, Gibco) in serum free medium for 1 h at 37 °C, according to the manufacturer's instruction ($n = 3$), followed by absorption measurement at 450 nm in ELISA microplate reader (BioTek, Republic of Korea). The values were normalized to that of the corresponding CB group on Day 1.

Real Time Quantitative PCR and Immunocytochemistry

Total RNA was extracted from ES-MSCs by Trizol (Ambion, USA), following the manufacturer's instruction ($n = 3$), and the concentration was determined in NanoDrop™ 2000c Spectrophotometer (Thermo Fisher Scientific). cDNA was then produced by reverse-transcription with AccuPower CycleScript RT Premix (Bioneer, Republic of Korea), according to the manufacturer's instructions. Real time quantitative PCR (qPCR) in StepOne Plus Real Time PCR System (Applied Biosystems) was run using SYBR Green PCR mix (10 μ L, Thermo Fisher Scientific), cDNA (50 ng/20 μ L) and primer set (10 pmol) at 60 °C for annealing ($n = 3$), followed by melting curve analysis and GAPDH normalization. The values were analyzed by the relative quantification $2^{-\Delta\Delta C_t}$ method and were further normalized to that of the corresponding CB group to present the fold changes. Stemness markers include Kruppel-like factor 4 (KLF4), c-Myc, sex determining region Y-box 2 (SOX2), and homeobox protein nanog (NANOG). Antioxidative activity markers include apurinic/aprimidinic endonuclease 1

TABLE 1. Lists of primer sequences.

	Primer sequence (5'–3')
hGAPDH	F-AACGAACGAGACTCTGGCAT R-ACCCGCACTTACTGGGAATT
hKLF4	F-TGTATTGAAGGATGGGAACCG R-AGTTCGTCTTTTCTGGGC
h c-Myc	F-ATGCCCTCAACGTTAGCTT R-TGCTGCTGCTGGTAGAAGT
hSOX2	F-AACCAAGACGCTCATGAAGA R-GCGAGTAGGACATGCTGTAG
hNANOG	F-ATAGCAATGGTGTGACGCGAG R-GATTGTTCCAGGATTGGGTG
hAPEX1	F-CAATACTGGTCAGCTCCTTC R-CAAATTCAGCCACAATCACC
hSENS1	F-AGATGAGGCAGTTACAGGAA R-ATGACGAGATACAGCTCTTG
hSOD2	F-CCTGGAACCTCACATCAACG R-GCTATCTGGGCTGTAACATC
hTXN	F-CGTGGCTGAGAAGTCAACTA R-ATCCATTTCCATCGGTCCCTT
ms-GAPDH	F-ATGTGTCGTTGGATCTGA R-TGCCTGCTTACCACCTTCT
ms IL-10	F-CTCCTTGATTTCTGGGCCAT R-ACTGGCATGAGGATCAGCAG
ms IL-6	F-AAGTGCATCATCGTTGTTATACA R-CAGGATACCACTCCCAACAGACC
ms IL-1b	F-GCCACCTTTTGACAGTGACAGTGATGAG R-ATCAGGACAGCCAGGTCAA

(APEX1), scalp-ear-nipple syndrome (SENS1), superoxide dismutase 2 (SOD2), and thioredoxin (TXN). Primer sequences are listed in Table 1.

Cells were fixed with 4% paraformaldehyde (Sigma-Aldrich), permeabilized and blocked using 0.3% Triton X-100 (Sigma-Aldrich) and 5% bovine serum albumin (Sigma-Aldrich) in PBS for 1 h at RT. Samples were treated with primary antibodies of CD146 (1:250, Abcam) in the blocking solution for 4 h at RT and then with the secondary antibodies of Rabbit IgG^{PE} (1:100, Abcam) for 1 h at RT, followed by counterstaining of actin and nuclei with phalloidin 488 (1:1000, Abcam) and NucBlue Fixed Cell ReadyProbes Reagent (Thermo Fisher Scientific), respectively. Samples were imaged by LSM700 confocal microscopy (Carl Zeiss, Germany).

In Vitro Tube Formation on Matrigel and Anti-inflammatory Activity

ES-MSCs were cultured on CB or FNGP for 4 days, and *in vitro* tubular formation of red fluorescent protein (RFP)-expressing human umbilical vein endothelial cells (HUVEC^{rfp}, 5x) was determined on Matrigel at Day 7 in co-culture with ES-MSC (1:1 seeding ratio with 5×10^5 cells/mL of each cell type) ($n = 3$), followed by imaging with fluorescence and light microscopy.

Anti-inflammatory activities of ES-MSCs post on CB or FNGP were determined against the activated macrophages (Raw 264.7). Raw cells without coculture (raw only) were used as a negative control. Raw 264.7 cells (1×10^5 cell/mL) were cultured at the bottom of trans-well plate for 1 day, followed by LPS treatment for 1 day. ES-MSCs (5×10^5 cell/mL) were cultured on CB plate and FNGP for 4 days. Then, ES-MSCs (1×10^4 cell/mL) was transferred in trans-well and attached for 1 day, followed by co-culture placement of ES-MSCs into the corresponding trans-well for 4 days. Gene expression of anti-(IL-10) and pro-(IL-6) inflammatory cytokines was assessed *via* qPCR. Secretion of these cytokines into the culture media was measured on Days 1 and 4 post-coculture using an ELISA kit (Abcam), according to the manufacturer's instructions.

Rescue of Mouse Hindlimb Ischemia by ES-MSCs

All procedures were approved under IACUC of Yonsei University College of Medicine. BALB/c nude mice (7-week old female) with 24–26 g were purchased from Orient-bio (Republic of Korea) and anesthetized by an intraperitoneal injection of zoletil and rompun. Their proximal and deep femoral artery and vein were tied with a 6–0 silk suture (Ethicon Inc., USA), and the blood vessels between the knots were completely cut to prevent the blood flow, thereby inducing tissue ischemia ($n = 5$).¹⁴ ES-MSCs were embedded in 5.5% gelatin hydrogels (Diameter = 5 mm) post-culture on CB or FNGP for 4 days and implanted into femoral muscle under ischemia. Sham (on surgery) and vehicle (gelatin only) groups served as controls. The animals were maintained for 2 weeks until euthanasia by CO₂ inhalation.

Blood flow patency in ischemic and normal hindlimbs was visualized by Laser Doppler Perfusion imaging (Moor instrument, USA) by capturing images of limbs on Days 0, 7, and 14 post-surgery with implantation, followed by computing the ratio of blood flow in ischemia(left) to normal(right). Histological examination of harvested hindlimbs was conducted by fixing with 10% formalin (Biosesang, Republic of Korea); embedding in paraffin wax; sectioning into 4 μ m thick slices; and staining with Mason's Trichrome, followed by imaging with light microscope (Leica).

Statistical Analysis

The quantitative data were expressed as the mean \pm standard deviation (SD). Statistical comparisons were made using two-way analysis of variance (ANOVA) with Bonferroni's *post hoc* analysis when

groups were compared with respect to more than one measurement factor and more than two nominal factors (SPSS 15.0; SPSS Inc.). One-way ANOVA was used when two or more groups were compared with respect to one measurement factor and one nominal factor (SPSS 15.0; SPSS Inc.). When only two groups were compared, the two-sample *t* test was used (SPSS 15.0; SPSS Inc.). *p* values were considered to indicate minimum statistical significance as shown in figures and legends.

RESULTS AND DISCUSSION

Characterization of ES-MSCs

Human adipose-derived mesenchymal stem cells (ADSCs, passage 2) and ES-MSCs (passage 10 and 11) were cultured on TCPS and CB, respectively, and they presented similar morphologies with adherent spreading and sporadic clustering, indicating typical MSC characteristics (Fig. 1). This result was supported by

flow cytometry analysis as the expression of MSC-positive markers (CD44 and CD73) was greater than 90% in both MSC types; whereas, the negative markers (CD34, CD11b, CD19, CD45 and HLA-DR) collectively were below 2% in both cell types.

Since fetal bovine serum (FBS) cannot be used for clinical trials owing to the risk of immune response,¹³ the CB plate was used to culture ES-MSCs. Nevertheless, this plate is expensive and unscalable for mass production as well as untunable for cell type-specific customization. Hence, this study aims to address this issue by affirming the enhanced therapeutic potential of ES-MSCs post-culture on a new coating alternative, thereby enabling mass production and serum-free process for clinical translation. We confirmed similar characteristics during expression of MSC markers with adhesion morphologies between ADSCs and ES-MSCs as the commencing point. ADSCs were selected as a control MSC type because of easy isolation in larger amounts,⁴ and thus, are considered as a preferred model for comparison with ES-MSCs. Moreover, ADSCs shared therapeutic properties with bone mar-

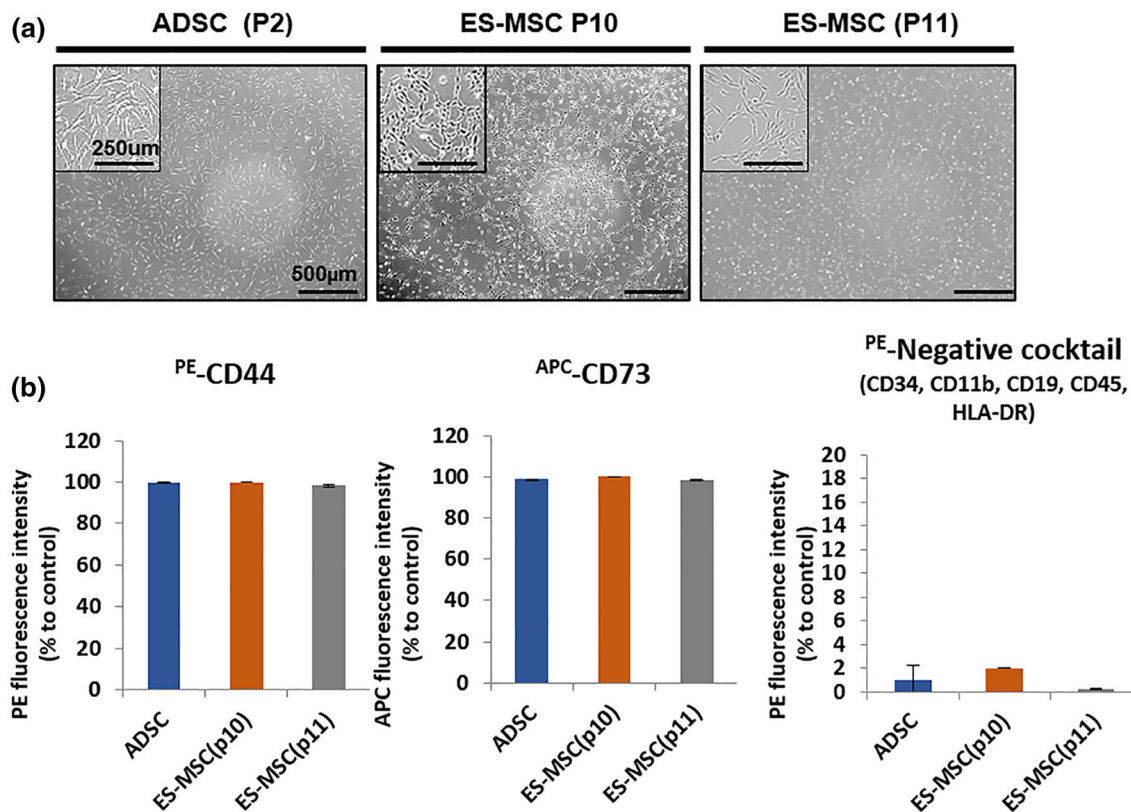


FIGURE 1. Characterization of human ES-MSC compared with human ADSC on Day 4 after cell seeding. Phase contrast images with magnification in the boxes (top left) and surface marker analysis *via* flow cytometry. No visible difference in adhesion and population of (a) ADSCs (passage 2), (b) ES-MSCs (passage 10) and (c) ES-MSCs (passage 11). (d) All MSC types are positive to CD44 (> 98%) and CD73 (> 99%), and negative (< 2%) to the combination of CD34, CD11b, CD19, and CD45.

row-derived MSCs in terms of anti-inflammatory and proangiogenic functions through paracrine effects.²

Cell Growth and Stemness on Test Coating Plates

The test coating plates were designed to enhance the cell binding affinity comparable to the commercial CB plate by combining fibronectin (FN) coating with PHSRN (FNP), gelatin (FNG), or both (FNGP) on tissue culture polystyrene (TCP). When ES-MSCs were cultured on the test coating plates for 7 days, the FNGP group revealed the most progressive increase in the cell population and spread with least cell clustering compared to the other groups (Fig. 2a). This result was supported by more detailed visualization by staining of actin cytoskeleton and nuclei. Cell aggregation and empty plate space were barely observed in the FNGP owing to uniform filling in contrast to the cell spindle and clustering morphologies of the other test groups accompanying progressive increases of empty plate spaces (Fig. 2b). These results indicate the synergistic affinity effect of FN and PHSRN on the efficient growth of ES-MSCs. Indeed, proliferation of MSC-ESCs was supported most effectively by the FNGP group for 7 days although ES-MSCs grew progressively from day 1 to 7 regardless of the test groups (Fig. 2c). In this study, FN was chosen after the use of PHSRN was planned following a previous study³ because the combination of PHSRN with RGD increased the FN affinity drastically compared to RGD alone. Other ECM molecules such as collagen and laminin also rely on RGD dominantly to maintain their affinity. Hence, FN served as a model component representing an adhesive RGD partner with PHSRN rather than the exclusive selection among others. A future study will investigate other ECM components to determine the affinity effect in the copresence with PHSRN and to compare with that of FN. A previous study⁵ demonstrated cell adhesion decreased significantly when a partner integrin was blocked using anti-integrin alpha 5 or anti-integrin beta 1 antibody in the copresence with PHSRN. This study also confirmed cells did not attach or spread when a scrambled peptide (HRPSN) was used instead of PHSRN. The results of this previous study indicate the RGD-specific integrin-dependent and the PHSRN sequence-specific mechanisms of the affinity effect. Gelatin was used as a coating bed to mix the affinity components because it helps regain PHSRN peptide and FN like an ECM function to deposit paracrine factors over the culture period.

Healthy, undifferentiated stem cells maintain high stemness, and there is a consensus that proliferating stem cells minimize differentiation and vice versa to pour their energy into one action. The expression levels

of stemness marker genes (KFL4, c-Myc, and NANOG) were highest in the FNGP group among the test groups on the 4th day of culture (Fig. 3a). Compared to the FNP and FNG groups, the CB group presented higher expression levels of c-Myc and NANOG, indicating its second efficient position in maintaining stemness during culture. Interestingly, SOX2 expression was highest in the FN group and even higher in the CB group compared to the FNP, FNG, and FNGP groups. SOX2 is a marker of pluripotency,³⁵ and thus, the results indicate that the FNGP supported the transition of pluripotency to multipotency of ES-MSCs while effectively maintaining other MSC-specific characteristics among the test groups.

Residual reactive oxygen species (ROS) are accumulated in unhealthy stem cells and damage the intracellular functions (“oxidative stress”), resulting in cell senescence.^{11,20} In contrast, healthy stem cells activate the antioxidative mechanisms against oxidative stress, thereby maintaining their stemness. APEX, SENS1, SOD2, and TXN are representative enzymes that involve ROS metabolism. Their expression levels were higher in the FNGP group compared to the CB group, indicating efficient support of FNGP to maintain a young, healthy status of ES-MSCs (Fig. 3b). Since the FNGP and CB groups were highly efficient in maintaining the expression of stemness markers, only these two groups were compared by excluding the other test groups. This result was supported by the expression of CD146 protein, that is, a marker of antioxidative activity and stemness (Fig. 3c).¹²

Collectively, the results proved the efficacy of FNGP over the commercial control, justifying a need to investigate the culture effect on the therapeutic functions of ES-MSCs as presented in the following experiments. The results also indicate a possibility to promote spontaneous differentiation of ES to MSC by controlling the matrix affinity as evidenced by the reduced expression of pluripotency marker with preservation of MSC characteristics and adhesive growth, which requires extensive further studies. This study adds a clear value to the field by demonstrating a case to customize the affinity of culture plate and thereby to enhance stemness of target cell type. In this way, a new type of scalable culture platform can be produced with improved cost-efficiency in the future.

In Vitro Proangiogenic and Anti-inflammatory Effects

Since the proangiogenic and anti-inflammatory functions of MSCs have been well elucidated, these aspects of ES-MSC function were investigated. Tube formation of red fluorescent human umbilical vein endothelial cells (HUVECs^{rfp}) was determined on Matrigel for 7 days by coculturing with ES-MSCs on

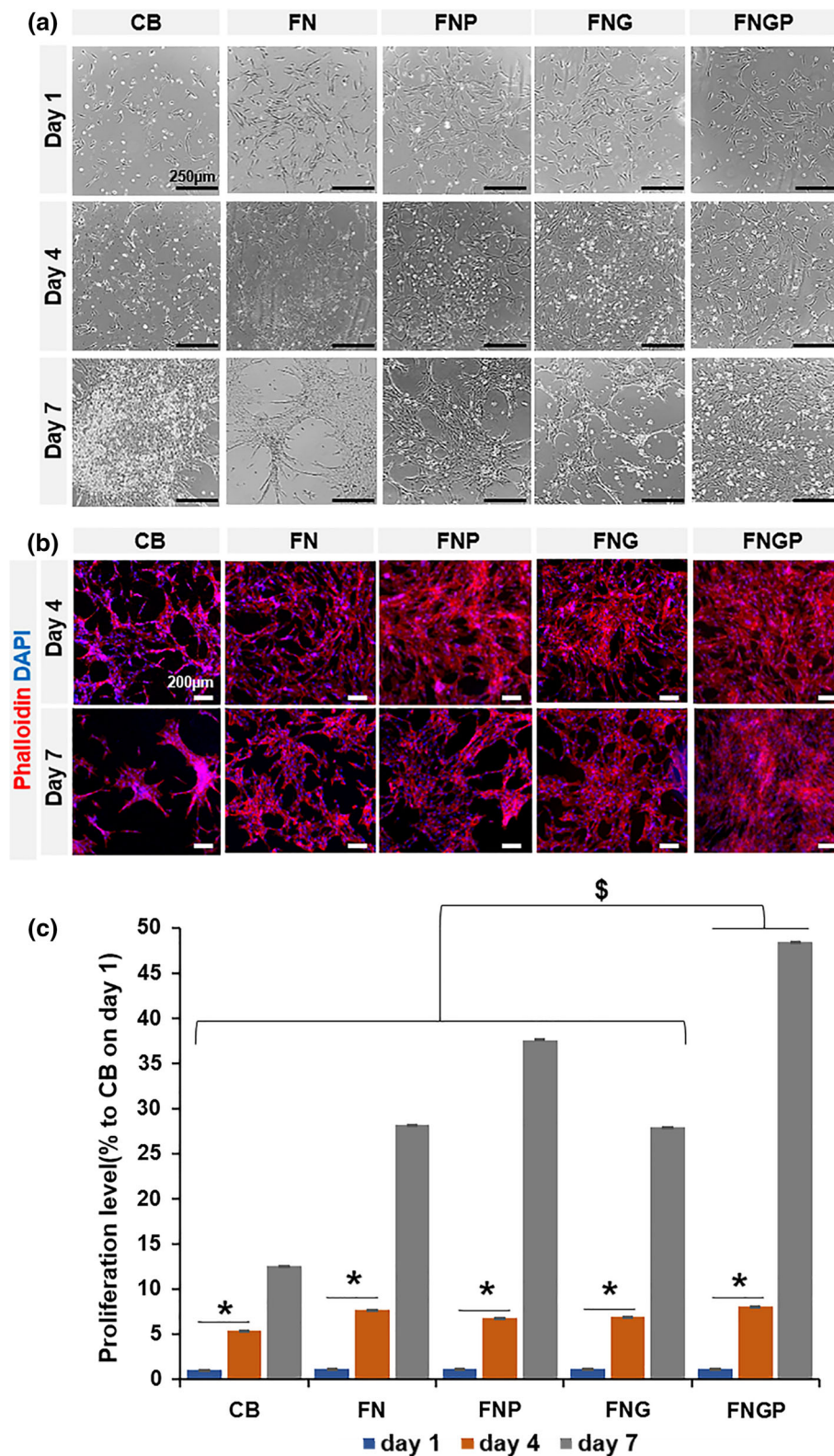


FIGURE 2. Spreading and proliferation of ES-MSC at Days 1, 4, and 7 post-culture on CellBind® (CB) in comparison to coating the tissue culture plate polystyrene (TCPS) with fibronectin only (FN), fibronectin and gelatin (FNG), fibronectin and PHSRN (FNP), and fibronectin, gelatin, and PHSRN (FNGP). (a) Phase contrast images of cell spreading morphologies, (b) fluorescent images of phalloidin (red) actin structures with counter nucleus (DAPI: blue) staining, and (c) analysis of progressive changes in cell proliferation. Graphs are presented in means \pm standard deviation (SD). * $p < 0.05$ Day1/4 vs. Day 7; and $^{\$}p < 0.05$ the other groups vs. FNGP group in both one-way and two-way ANOVA tests ($n = 3$).

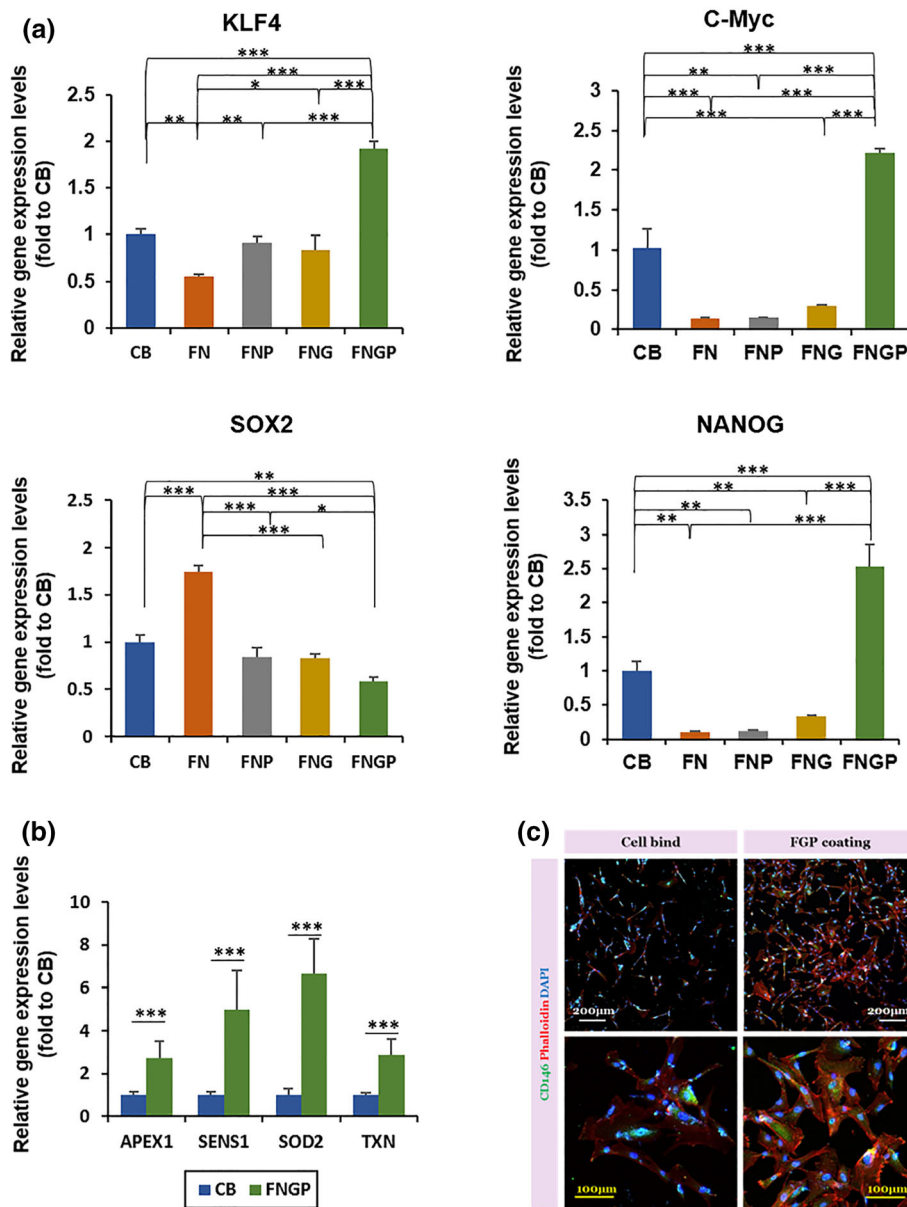


FIGURE 3. Expression of stemness and antioxidant activity markers on Day 4 post-culture of ES-MSCs on CB, FN, FNG, FNP, and FNGP. Gene expression of (a) stemness markers (Klf4, c-Myc, SOX2, and NANOG) and (b) antioxidant activity markers (APEX, SENS1, SOD2, and TXN) by real time qPCR. Samples were normalized to GAPDH expression (house-keeping gene). At least three independent experiments were performed in triplicates. Graphs are presented as average \pm SD. * $p < 0.05$, ** $p < 0.01$ and *** $p < 0.001$ between the line connected groups in one-way and two-way ANOVA tests or t test ($n = 3$). (c) CD146 immunostaining evaluates both stemness and antioxidant activity.

Day 4 post-culture on CB (MSC_{CB}) vs. FNGP (MSC_{FNGP}; Fig. 4). The HUVEC group (without coculture) served as a control. The results from early tube formation at 3, 6, and 12 h post-seeding and late tube formation at 1, 4, and 7 days post-seeding were visualized *via* phase contrast and confocal fluorescence imaging. During early time period, the HUVEC group maintained a typical pattern in tube formation, whereas the coculture groups appeared to promote tube thickness with cell clustering at branch points

(Fig. 4a). The HUVEC group pattern prolonged to the late time period, and more tube formation (white arrows) points were observed in the MSC_{FNGP} group compared to the MSC_{CB} group (Fig. 4b), indicating an enhanced proangiogenic activity by culturing ES-MSCs on FNGP over CB, which agrees to the aforementioned results.

Furthermore, anti-inflammatory activities of ES-MSCs were determined post-culture on CB or FNGP considering the regulatory cytokine production of

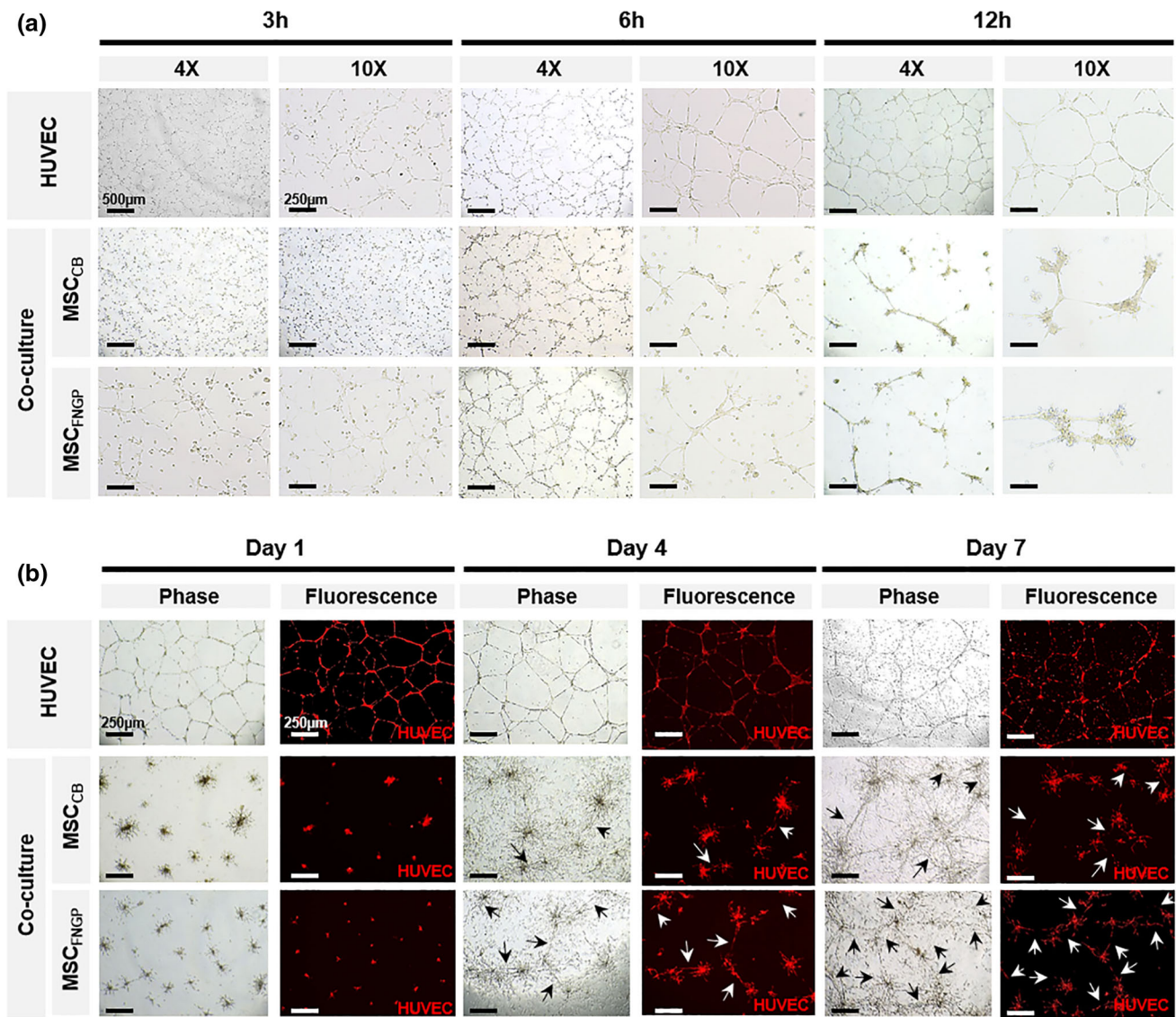


FIGURE 4. Tube formation of HUVEC^{rfp} (red) on Matrigel for 7 days in coculture with ES-MSCs on Day 4 post-culture on CB (MSC_{CB}) vs. FNGP (MSC_{FNGP}). HUVEC group (without coculture) served as a control. (a) Early tube formation at 3, 6, and 12 h post-seeding and (b) late tube formation at 1, 4, and 7 days post-seeding were visualized *via* phase contrast and confocal fluorescence imaging.

activated macrophages (Raw 264.7; Fig. 5). Raw 264.7 mouse macrophages were activated by 1 day LPS treatment after preculturing at the bottom of a trans-well plate for 1 day and were then subjected to coculture placement of ES-MSCs into the corresponding trans-well for 4 days (Fig. 5a). The activated macrophage group without coculture (raw only) was used as a negative control. The gene expression levels of anti-inflammatory cytokine (IL-10) in both coculture groups significantly increased from Days 4–7, and the level of CB group was higher than those of FNGP and raw only groups at both time periods (Fig. 5b-i). In contrast, compared to the raw only group, the gene expression levels of pro-(IL-6) inflammatory cytokines

in both coculture groups were lower on Day 4 and increased to the higher levels on Day 7. The level of FNGP group was significantly lower than that of the CB group on Day 7 (Fig. 5b-ii), suggesting FNGP as a culture matrix candidate to reduce detrimental proinflammatory actions.

As the IL-10 gene was expressed more in the CB group than the FNGP group, the release of both cytokines was determined by ELISA using a culture media (Fig. 5c). Only FNGP group revealed a significant increase in the anti-inflammatory IL-10 secretion from Days 4–7, and their levels were maintained higher than those of CB and raw only groups (Fig. 5c-i). The secretion level of proinflammatory IL-6 significantly

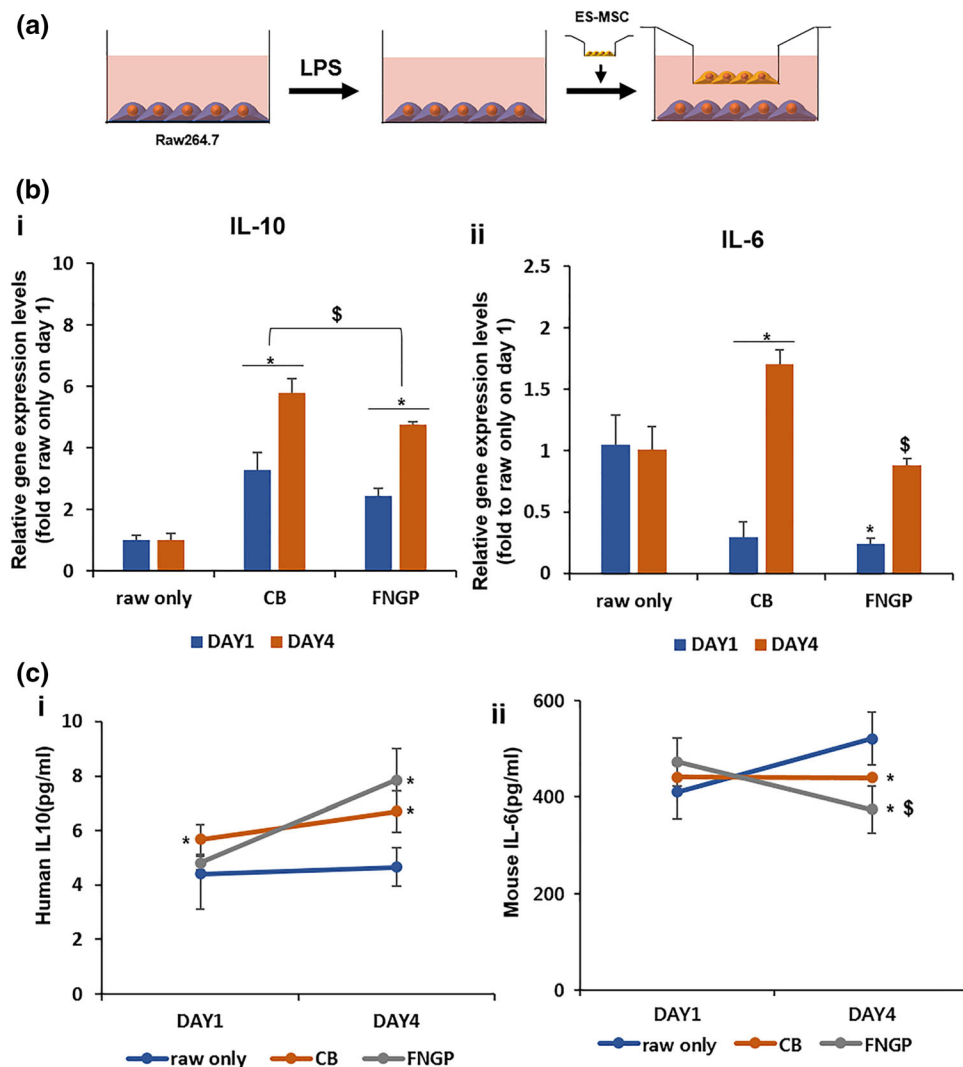


FIGURE 5. Anti-inflammatory activity of ES-MSCs on CB or FNGP against activated macrophages (Raw 264.7). Raw cells without coculture (raw only) were used as a control. (a) Schematic illustration of experimental procedure for 1 day treatment of LPS to Raw 264.7 mouse macrophages after preculturing at the bottom of trans-well plate for 1 day, followed by coculture placement of ES-MSCs into the corresponding trans-well for 4 days. (b) Gene expression and (c) protein secretion of anti-(IL-10) and pro-(IL-6) inflammatory cytokines by qPCR and ELISA, respectively. All results are presented as means \pm SD. The qPCR results were normalized to GAPDH gene expression. * $p < 0.05$ vs. raw only; and $^{\S}p < 0.05$ vs. CB in both one-way and two-way ANOVA tests ($n = 3$).

decreased in the FNGP group from Day 1 to 4 as in contrast to the CB group. On Day 4, the level of FNGP group was significantly lower compared to the raw only and CB groups (Fig. 5c-ii).

These results support the FNGP in improving the therapeutic function of ES-MSCs *via* enhancement of proangiogenic and anti-inflammatory activities. The FNGP serves as a promising platform for treating ischemic diseases by promoting vascular perfusion and by attenuating detrimental macrophage behavior.^{15,16} Moreover, the patterns of cytokine production suggest an underlying mechanism to induce the proangiogenic M2 phenotype (IL-10) of macrophages while reducing the detrimental M1 phenotype (IL-6), although pro-

filin a wider range of cytokine release is required to reach this conclusion through further studies.

Rescue of Mouse Ischemic Hindlimb

Since culturing ES-MSCs on FNGP promoted proangiogenic and anti-inflammatory activities, these therapeutic functions were tested in a mouse model with hindlimb ischemia. After culturing on FNGP or CB for 4 days, ES-MSCs were embedded in gelatin hydrogels (1×10^6 cells/ $20 \mu\text{L}$ of 5.5% gelatin), which were then intramuscularly implanted into femoral muscle of the ischemic hind-limb for 2 weeks (Fig. 6). Sham (on surgery) and vehicle (gelatin only) groups

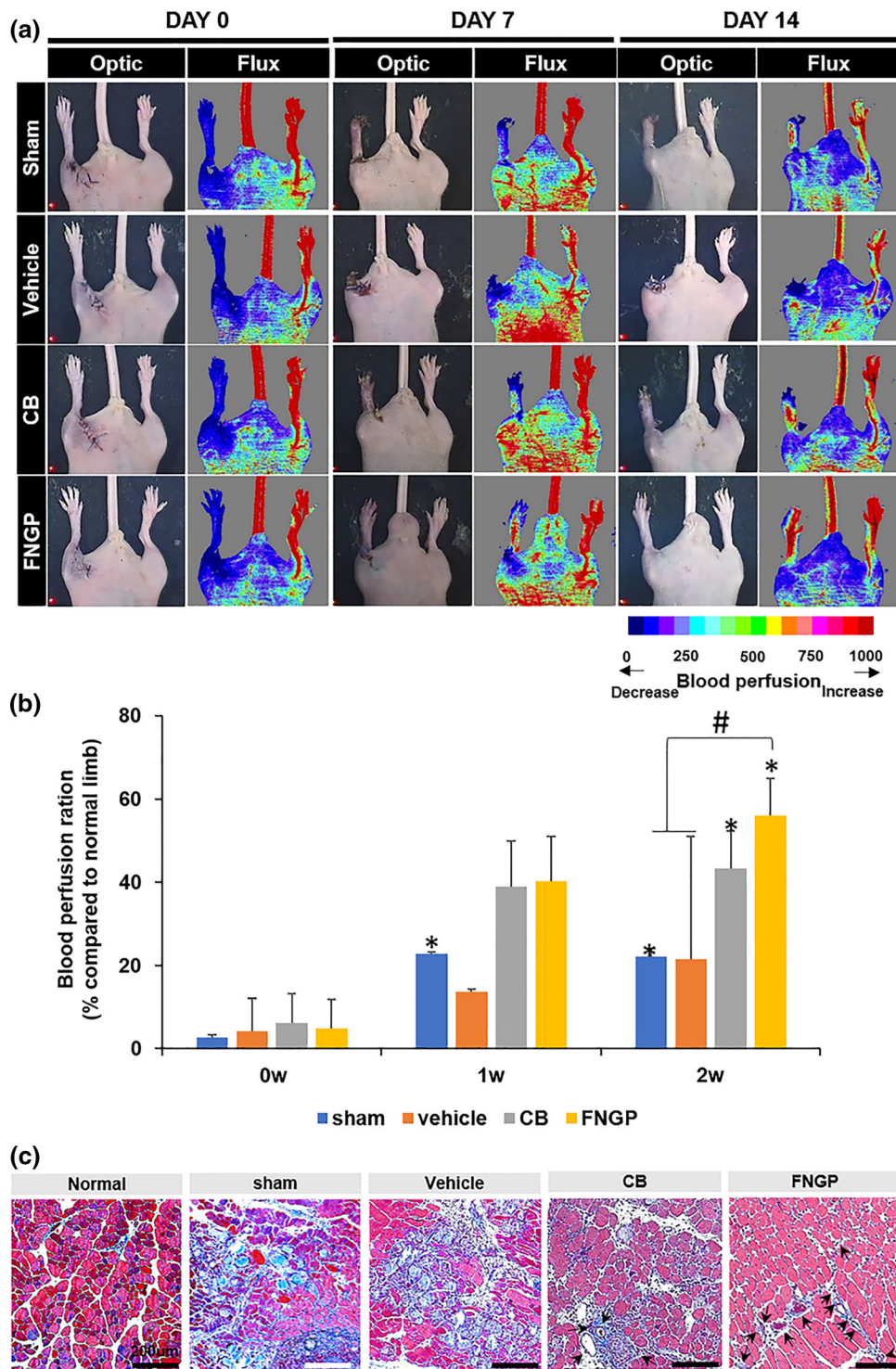


FIGURE 6. Rescue of mouse ischemic hindlimbs by implantation of gelatin hydrogels with ES-MSCs post-culture on CB or FNGP. (a) The laser doppler (right) and optic (left) images on Days 0, 7, and 14 post-surgery with implantation. Color scale indicates blood perfusion range from minimum (blue) to maximum (red). (b) Quantitative analysis of LDPI results by computing the ratio of blood flow in ischemia (left) to normal (right). * $p < 0.05$ vs. FNGP; and * $p < 0.05$ vs. 0 w within the same group in both one-way and two-way ANOVA tests ($n = 5$). (c) Masson’s trichrome staining of ischemic muscle on Day 14 post-surgery with implantation (black arrow: blood vessel).

served as controls. Laser Doppler images of sham and vehicle groups presented gradual limb loss, eventually to severe degrees from days 0–14, indicating successful modeling of hindlimb ischemia in mice (Fig. 6a). In contrast, the CB and FNGP groups rescued the limb loss visibly due to the recovered patency of blood perfusion up to about 56% of the normal limb (Fig. 6b). The FNGP group presented accelerated and full perfusion patency throughout the limb including the extreme distal part, whereas only proximal perfusion with slower recovery was observed in the CB group.

Moreover, the images of Masson's trichrome staining presented blood vessels (black arrows), inflammatory cell invasion (dark purple dots), and tissue fibrosis (sky blue) (Fig. 6c). More fibrotic tissue formation and inflammatory cell invasion were present in the sham and vehicle groups presumably owing to the lack of blood vessels compared to the normal, CB, and FNGP groups. The FNGP group exhibited visibly limited formation of fibrotic tissues with abundant presence of blood cells as an evidence of rich vessel formation in contrast to the spreading signals of fibrotic tissue with a relatively small population of blood cells in the CB group. These results prove the promising therapeutic function of FNGP group in rescuing the damaged tissues of mouse ischemic limb.

Preservation of high stemness with minimum spontaneous differentiation has been crucial in propagating stem cells to attain a clinical dose. Moreover, commercial plates are neither tunable nor scalable for stem cell type-specific customization. This study suggests a promising solution to address these issues by simply tuning the affinity of culture plate. As a result, FNGP played a key role in promoting the value of ES-MSCs as an alternative of adult MSCs from bench to clinical transition. Proangiogenic²⁷ and anti-inflammatory⁷ functions were improved by culturing ES-MSCs on FNGP, and thus their therapeutic potential to rescue ischemic hindlimbs was affirmed *in vivo*. The therapeutic potential of MSCs was well studied,^{25,30} and their paracrine effects were recognized as the main mechanism.^{28,29} Nevertheless, further studies are required to prove this point because therapeutic actions of MSCs are dependent on their tissue of origin. Their main mechanisms to promote blood vessel formation include paracrine effects,²⁰ endothelial differentiation,¹⁸ and pericyte function³⁴; however, MSC type-dependent alternation of these mechanisms remains unclear. Hence, the next study is underway to investigate a regenerative mechanism of ES-MSCs.

CONCLUSION

The use of animal serum as common supplements for the expansion of MSCs has been issued for clinical studies due to the safety concerns involved. Ideal culture of MSCs should allow for achieving the clinically relevant cell number by supporting efficient proliferation with minimum passage numbers, thereby reducing cell senescence and relevant abnormalities during *ex vivo* expansion. Significance of this study lies in the fact that the FNGP template can serve as an alternative of the commercial plate with essential benefits including cost efficiency, tunable adhesiveness, xenofreeness, and scalable coating. More importantly, the idea to promote the therapeutic potential of ES-MSCs while culturing adds a clear value to the relevant research fields by addressing the long-standing issue during exhausted expansions.

ACKNOWLEDGMENTS

H. S. Kim and S. H. Choi contributed equally to this work and are thus listed as the equal first authors. We acknowledge Dr. Dae-Hyun Kim for guiding mouse experiments.

AUTHOR CONTRIBUTIONS

H-J.S. and K.N.K conceived and initiated the entire study. H-S.K. and S.H.C conducted most experiments. M-L. K designed the experiments and analyzed the results. H-S.K., S.H.C., M-L. K., and K-W. L wrote the paper. H-J.S. and K.N.K supervised all aspects of the study.

FUNDING

This work was financially supported by DAE-WOONG Pharmaceutical and the National Research Foundation of Korea (NRF) (2016M3A9E9941743 and 2019R1A2C2010802).

DATA AVAILABILITY

The data used to support the findings of this study are included within the article.

CONFLICT OF INTEREST

Hye-Seon Kim, Sung Hyun Choi, Mi-Lan Kang, Ki-Won Lee, Ki Nam Kim and Hak-Joon Sung have

no known conflicts of interest or significant financial support associated with this publication that could have influenced its outcome.

ETHICAL APPROVAL

All animal studies were carried out in accordance with the Guide for the Care and Use of Laboratory Animals (NIH publication No. 85–23 revised 1985) and approved by IACUC. No human studies were carried out by the authors for this publication.

REFERENCES

- ¹Bianco, P., X. Cao, P. S. Frenette, J. J. Mao, P. G. Robey, P. J. Simmons, and C. Y. Wang. The meaning, the sense and the significance: translating the science of mesenchymal stem cells into medicine. *Nat. Med.* 19(1):35–42, 2013.
- ²Bronckaers, A., P. Hilkens, W. Martens, P. Gervois, J. Ratajczak, T. Struys, and I. Lambrechts. Mesenchymal stem/stromal cells as a pharmacological and therapeutic approach to accelerate angiogenesis. *Pharmacol. Ther.* 143(2):181–196, 2014.
- ³Dankers, P. Y., M. C. Harmsen, L. A. Brouwer, M. J. van Luyn, and E. W. Meijer. A modular and supramolecular approach to bioactive scaffolds for tissue engineering. *Nat. Mater.* 4(7):568–574, 2005.
- ⁴De Francesco, F., G. Ricci, F. D'Andrea, G. F. Nicoletti, and G. A. Ferraro. Human adipose stem cells: from bench to bedside. *Tissue Eng. Part B Rev.* 21(6):572–584, 2015.
- ⁵Feng, Y., and M. Mrksich. The synergy peptide PHSRN and the adhesion peptide RGD mediate cell adhesion through a common mechanism. *Biochemistry* 43(50):15811–15821, 2004.
- ⁶Giam, L. R., M. D. Massich, L. Hao, L. Shin Wong, C. C. Mader, and C. A. Mirkin. Scanning probe-enabled nanocombinatorics define the relationship between fibronectin feature size and stem cell fate. *Proc. Natl. Acad. Sci. USA* 109(12):4377–4382, 2012.
- ⁷Hamidian Jahromi, S., C. Estrada, Y. Li, E. Cheng, and J. E. Davies. Human umbilical cord perivascular cells and human bone marrow mesenchymal stromal cells transplanted intramuscularly respond to a distant source of inflammation. *Stem Cells Dev.* 27(6):415–429, 2018.
- ⁸Hawkins, K. E., M. Corcelli, K. Dowding, A. M. Ranzoni, F. Vlahova, K. L. Hau, A. Hunjan, D. Peebles, P. Gressens, H. Hagberg, P. de Coppi, M. Hristova, and P. V. Guillot. Embryonic stem cell-derived mesenchymal stem cells (MSCs) have a superior neuroprotective capacity over fetal MSCs in the hypoxic-ischemic mouse brain. *Stem Cells Transl. Med.* 7(5):439–449, 2018.
- ⁹Hematti, P. Human embryonic stem cell-derived mesenchymal progenitors: an overview. *Methods Mol. Biol.* 690:163–174, 2011.
- ¹⁰Huang, G. S., L. G. Dai, B. L. Yen, and S. H. Hsu. Spheroid formation of mesenchymal stem cells on chitosan and chitosan-hyaluronan membranes. *Biomaterials* 32(29):6929–6945, 2011.
- ¹¹Ji, A. R., S. Y. Ku, M. S. Cho, Y. Y. Kim, Y. J. Kim, S. K. Oh, S. H. Kim, S. Y. Moon, and Y. M. Choi. Reactive oxygen species enhance differentiation of human embryonic stem cells into mesendodermal lineage. *Exp. Mol. Med.* 42(3):175–186, 2010.
- ¹²Jin, H. J., J. H. Kwon, M. Kim, Y. K. Bae, S. J. Choi, W. Oh, Y. S. Yang, and H. B. Jeon. Downregulation of melanoma cell adhesion molecule (MCAM/CD146) accelerates cellular senescence in human umbilical cord blood-derived mesenchymal stem cells. *Stem Cells Transl. Med.* 5(4):427–439, 2016.
- ¹³Kandoi, S., L. Praveen-Kumar, B. Patra, P. Vidyasekar, D. Sivanesan, S. Vijayalakshmi, K. Rajagopal, and R. S. Verma. Evaluation of platelet lysate as a substitute for FBS in explant and enzymatic isolation methods of human umbilical cord MSCs. *Sci. Rep.* 8(1):12439, 2018.
- ¹⁴Kang, K. T., R. Z. Lin, D. Kuppermann, J. M. Melero-Martin, and J. Bischoff. Endothelial colony forming cells and mesenchymal progenitor cells form blood vessels and increase blood flow in ischemic muscle. *Sci. Rep.* 7(1):770, 2017.
- ¹⁵Kao, W. J., and D. Lee. In vivo modulation of host response and macrophage behavior by polymer networks grafted with fibronectin-derived biomimetic oligopeptides: the role of RGD and PHSRN domains. *Biomaterials* 22(21):2901–2909, 2001.
- ¹⁶Kao, W. J., D. Lee, J. C. Schense, and J. A. Hubbell. Fibronectin modulates macrophage adhesion and FBGC formation: the role of RGD, PHSRN, and PRRARV domains. *J. Biomed. Mater. Res.* 55(1):79–88, 2001.
- ¹⁷Kimura, K., A. Hattori, Y. Usui, K. Kitazawa, M. Nagamura, K. Kawamoto, S. Teranishi, M. Nomizu, and T. Nishida. Stimulation of corneal epithelial migration by a synthetic peptide (PHSRN) corresponding to the second cell-binding site of fibronectin. *Invest. Ophthalmol. Vis. Sci.* 48(3):1110–1118, 2007.
- ¹⁸Lee, S. H., Y. Lee, Y. W. Chun, S. W. Crowder, P. P. Young, K. D. Park, and H. J. Sung. In situ crosslinkable gelatin hydrogels for vasculogenic induction and delivery of mesenchymal stem cells. *Adv. Funct. Mater.* 24(43):6771–6781, 2014.
- ¹⁹Mackensen, A., R. Drager, M. Schlesier, R. Mertelsmann, and A. Lindemann. Presence of IgE antibodies to bovine serum albumin in a patient developing anaphylaxis after vaccination with human peptide-pulsed dendritic cells. *Cancer Immunol. Immunother.* 49(3):152–156, 2000.
- ²⁰Maraldi, T., C. Angeloni, E. Giannoni, and C. Sell. Reactive oxygen species in stem cells. *Oxid. Med. Cell Longev.* 2015:159080, 2015.
- ²¹Martin, M. J., A. Muotri, F. Gage, and A. Varki. Human embryonic stem cells express an immunogenic nonhuman sialic acid. *Nat. Med.* 11(2):228–232, 2005.
- ²²Mendicino, M., A. M. Bailey, K. Wonnacott, R. K. Puri, and S. R. Bauer. MSC-based product characterization for clinical trials: an FDA perspective. *Cell Stem Cell* 14(2):141–145, 2014.
- ²³Park, Y. H., J. I. Yun, N. R. Han, H. J. Park, J. Y. Ahn, C. Kim, J. H. Choi, E. Lee, J. M. Lim, and S. T. Lee. Mass production of early-stage bone-marrow-derived mesenchymal stem cells of rat using gelatin-coated matrix. *Biomed. Res. Int.* 2013:347618, 2013.
- ²⁴Rustad, K. C., V. W. Wong, M. Sorkin, J. P. Glotzbach, M. R. Major, J. Rajadas, M. T. Longaker, and G. C. Gurtner. Enhancement of mesenchymal stem cell angiogenic capacity and stemness by a biomimetic hydrogel scaffold. *Biomaterials* 33(1):80–90, 2012.
- ²⁵Smirnov, S. V., R. Harbacheuski, A. Lewis-Antes, H. Zhu, P. Rameshwar, and S. V. Kotenko. Bone-marrow-derived

- mesenchymal stem cells as a target for cytomegalovirus infection: implications for hematopoiesis, self-renewal and differentiation potential. *Virology* 360(1):6–16, 2007.
- ²⁶Swamynathan, P., P. Venugopal, S. Kannan, C. Thej, U. Kolkundar, S. Bhagwat, M. Ta, A. S. Majumdar, and S. Balasubramanian. Are serum-free and xeno-free culture conditions ideal for large scale clinical grade expansion of Wharton's jelly derived mesenchymal stem cells? A comparative study. *Stem Cell Res. Ther.* 5(4):88, 2014.
- ²⁷Tao, H., Z. Han, Z. C. Han, and Z. Li. Proangiogenic features of mesenchymal stem cells and their therapeutic applications. *Stem Cells Int.* 2016:1314709, 2016.
- ²⁸Tebebi, P. A., S. J. Kim, R. A. Williams, B. Milo, V. Frenkel, S. R. Burks, and J. A. Frank. Improving the therapeutic efficacy of mesenchymal stromal cells to restore perfusion in critical limb ischemia through pulsed focused ultrasound. *Sci. Rep.* 7:41550, 2017.
- ²⁹Teixeira, F. G., M. M. Carvalho, N. Sousa, and A. J. Salgado. Mesenchymal stem cells secretome: a new paradigm for central nervous system regeneration? *Cell. Mol. Life Sci.* 70(20):3871–3882, 2013.
- ³⁰Togel, F., Z. Hu, K. Weiss, J. Isaac, C. Lange, and C. Westenfelder. Administered mesenchymal stem cells protect against ischemic acute renal failure through differentiation-independent mechanisms. *Am. J. Physiol. Renal Physiol.* 289(1):F31–42, 2005.
- ³¹Tuschong, L., S. L. Soenen, R. M. Blaese, F. Candotti, and L. M. Muul. Immune response to fetal calf serum by two adenosine deaminase-deficient patients after T cell gene therapy. *Hum. Gene Ther.* 13(13):1605–1610, 2002.
- ³²Wang, J., J. Hao, D. Bai, Q. Gu, W. Han, L. Wang, Y. Tan, X. Li, K. Xue, P. Han, Z. Liu, Y. Jia, J. Wu, L. Liu, L. Wang, W. Li, Z. Liu, and Q. Zhou. Generation of clinical-grade human induced pluripotent stem cells in Xeno-free conditions. *Stem Cell Res. Ther.* 6:223, 2015.
- ³³White, S. Reflections upon caring for dying people. *Inforum* 12:27, 1991.
- ³⁴Wong, S. P., J. E. Rowley, A. N. Redpath, J. D. Tilman, T. G. Fellous, and J. R. Johnson. Pericytes, mesenchymal stem cells and their contributions to tissue repair. *Pharmacol. Ther.* 151:107–120, 2015.
- ³⁵Zhang, S., and W. Cui. Sox2, a key factor in the regulation of pluripotency and neural differentiation. *World J. Stem Cells* 6(3):305–311, 2014.

Publisher's Note Springer Nature remains neutral with regard to jurisdictional claims in published maps and institutional affiliations.